Available online at www.sciencedirect.com
ScienceDirect
Journal of Solid State Chemistry 181 (2008) 935–942
JOURNAL OF SOLID STATE CHEMISTRY
www.elsevier.com/locate/jssc

High surface area V–Mo–N materials synthesized from amine intercalated foams

Piotr Krawiec[a], Rabi Narayan Panda[b], Emanuel Kockrick[a], Dorin Geiger[c], Stefan Kaskel[a,*]

[a]Institute of Inorganic Chemistry, Technical University of Dresden, Mommsenstr. 6, D-01062 Dresden, Germany
[b]Birla Institute of Technology and Science, Pilani, Goa campus, NH 17 Bypass Road, Zuarinagar, Goa 403726, India
[c]Triebenberg Laboratory for HRTEM and Electron Holography, Institute for Structure Physics, Technical University of Dresden, Zum Triebenberg 50, 01328 Dresden, Germany

Received 10 May 2007; received in revised form 15 October 2007; accepted 6 January 2008
Available online 26 January 2008

Abstract

Nanocrystalline ternary V–Mo nitrides were prepared via nitridation of amine intercalated oxide foams or bulk ternary oxides. Specific surface areas were in the range between 40 and 198 $m^2 g^{-1}$ and strongly depended on the preparation method (foam or bulk oxide). Foamed precursors were favorable for vanadium rich materials, while for molybdenum rich samples bulk ternary oxides resulted in higher specific surface areas. The materials were characterized via nitrogen physisorption at 77 K, X-ray diffraction patterns, electron microscopy, and elemental analysis.

Keywords: Transition metal nitride; High surface area; Sol–gel; Oxide foam

1. Introduction

Transition metal nitrides and carbides have been studied intensively as electronic and structural ceramics [1–4]. Compared to oxides they have superior properties in some respects such as hardness, mechanical strength and high melting points [1]. As shown in the pioneering work of Levy and Boudart [5,6] and, more recently, summarized by Oyama [7,8] transition metal nitrides and carbides can also be efficient catalysts. In particular, compounds such as W_2N or Mo_2N have attracted attention as catalysts for hydrotreating reactions [9–11]. In oxidation, hydrogenation or isomerization reactions, the catalytic properties of the transition metal nitrides and carbides resemble those of the group VIII noble metals [5,6]. Thus, transition metal nitrides and carbides may offer a promising economic alternative to conventional noble metal catalysts. A key issue for improving this class of materials is the development of synthesis methods producing materials with high surface areas and particle sizes in the nanometer range [12–15]. Nanoparticles ($d<100$ nm) are also crucial in the preparation of dense materials, since they allow rapid densification at temperatures lower than required for micrometer-sized powders, and yield materials with enhanced plastic or superplastic properties [16–18].

Some studies have been reported on the synthesis and characterization of nanocrystalline high surface area binary and ternary nitrides containing V and Mo [19–23]. The idea is to modify the electronic structure of the materials by changing the composition of the ternary materials. Especially in solid solutions fine tuning of electronic properties is achieved with different composition. In addition, there can be a difference in the oxygen concentration, which can alter the electronic properties substantially. Oyama et al. have studied the preparation of high surface area bimetallic Mo–V oxy-nitrides, including their catalytic activities in hydrodesulfurization (HDS) and hydrodenitrogenation (HDN) reactions [24,25]. It has been shown that the HDS and HDN activities of the Mo–V bimetallic oxy-nitrides are enhanced compared to those of the binary nitride phases [24]. The materials were prepared by nitridation of V_2MoO_8 precursors which were obtained by conventional solid-state route. The highest value of the

*Corresponding author. Fax: +49 351 4633 7287.
E-mail address: stefan.kaskel@chemie.tu-dresden.de (S. Kaskel).

0022-4596/$ - see front matter © 2008 Elsevier Inc. All rights reserved.
doi:10.1016/j.jssc.2008.01.028

surface area obtained for one of these materials was $74\,m^2\,g^{-1}$ [24,25].

A common method for the preparation of binary and ternary transition metal nitrides is nitridation of binary and ternary oxides as well as metals or their alloys in ammonia flow at high temperatures (700–1000 °C) [8]. In order to obtain products with high specific surface area, extremely high ammonia space velocities are required [21]. Another possibility enhancing the specific surface area is the pre-structuring of precursor oxides. High surface area sol–gel derived foams are typically used as substrates [26] as well as freeze dried precursors and aeorgels [27,28]. We have shown that the nitridation of the amine intercalated V_2O_5 foams can yield VN with extraordinary high specific surface areas and small crystallites [29]. More recently, high surface area mesoporous carbon nitride exotemplate was found to be useful for the preparation of the transition metal nitride nanoparticles [30]. Such template functions on the same time as the nitrogen source [30,31]. Solid-state metathesis reactions were also employed for the preparation of transition metal nitrides [32].

In this work, ternary V–Mo nitrides were prepared using pre-structured foam precursors. We show that high surface area (up to $198\,m^2\,g^{-1}$) ternary nitrides can be effectively prepared via this procedure and we compare the surface areas to those of materials synthesized via direct nitridation of bulk ternary oxides.

2. Experimental

2.1. Preparation of ternary oxides

In the first, step ternary oxides were prepared in a solid-state reaction of appropriate amounts of MoO_3 (99.6 + % Aldrich) and V_2O_5 (99.6 + wt% Aldrich) (Scheme 1). The oxide powders were first ground in a mortar, and then heated in an alumina crucible at 700 °C for 2 h (heating ramp of of $5\,°C\,min^{-1}$).

2.2. Ternary nitrides via direct oxide nitridation

As prepared ternary oxides (1 g) were placed in the middle of the vertical quartz tube reactor (3 cm in diameter) on the quartz frit, and heated in ammonia flow ($1047\,cm^3\,min^{-1}$) from top to bottom to 800 °C with a heating ramp of $120\,°Ch^{-1}$. Subsequently, the furnace was cooled down to room temperature with $300\,°Ch^{-1}$. The product was passivated in the O_2/N_2 mixture (1% O_2).

2.3. Ternary nitrides via foam route

For the preparation of ternary foams, a modified synthesis of Chandrappa et al. was used [33–35]. As prepared ternary oxides (5 g) were mixed with 10 g of hexadecylamine (90% Aldrich) and 15 ml of acetone. The slurry was stirred until a pasty material formed (5–10 min) and subsequently, 250 ml of 30 wt% H_2O_2 solution was added. The foaming process started after few minutes and the product was spread onto a clean glass surface for overnight drying. The foam was placed in a vertical quartz tube reactor (diameter of 3 cm with a quartz frit in the middle) and heated in an ammonia flow of $170\,cm^3\,min^{-1}$ (from bottom to top) at a heating ramp of $120\,°C\,h^{-1}$ to 800 °C. The temperature was maintained for 2 h and then cooled down to room temperature with $300\,°C\,h^{-1}$. The product was passivated in the O_2/N_2 mixture (1% O_2).

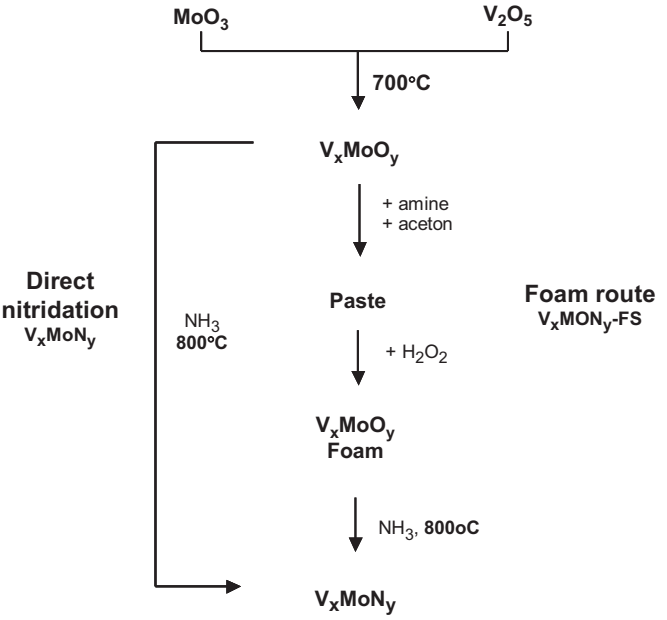

Scheme 1. Two preparation procedures of ternary nitrides (direct nitridation and foam route).

2.4. Characterization

Powder X-ray diffraction patterns were recorded in transmission geometry using a Stoe Stadi-P diffractometer and Cu $K\alpha_1$ radiation ($\lambda = 0.15405$ nm). The average crystallite size was calculated from the Scherrer equation (STOE Size/Strain analysis [36]). For the FWHM estimation, three reflections ((111), (200) and (220)) were fitted using a Pseudo–Voigt function. The instrumental peak broadening was calculated using LaB_6. Elemental analyses of carbon and nitrogen were performed via the combustion and hot gas extraction method. Nitrogen physisorption measurements were performed on a Quantachrome Autosorb 1C instrument. Prior to the measurements, the samples were evacuated at 150 °C for 5 h. The specific surface areas were calculated from the BET equation ($P/P_o = 0.1$–0.3). TEM investigations were performed on the Cs-corrected 200 kV TEM FEI Tecnai F20 Cs-corr at the Triebenberg-Laboratory for high-resolution TEM and electron holography. Cs-correction was used for a precise estimation of the lateral dimensions in order to avoid errors induced by delocalization effects caused by a high spherical aberration.

3. Results and discussion

In our previous work, the preparation of high specific surface area vanadium nitride via foam procedure was demonstrated [29]. In principle, such method can be extended to any other nitride and carbide materials if the corresponding oxides form foams in the presence of amines. For example, Arbatzis showed the same procedure can be easily applied to prepare TiO_2 foams [37]. However, our attempts to prepare the MoO_3 foam (via similar procedure) was not successful (probably due to low decomposition rate of H_2O_2 in presence of MoO_3), but we observed that it is possible to prepare foams from ternary oxides with a V/Mo ratio higher than one. In this paper, ternary nitrides with V/Mo ratio higher or equal to one are discussed. For comparison, binary (VN and Mo_2N) and ternary nitrides were also prepared via the direct nitridation route (Scheme 1).

V_xMoO_y substrates were prepared with different V/Mo ratios by heating appropriate amounts of V_2O_5 and MoO_3 precursors up to 700 °C and cooling down to room temperature. According to X-ray diffraction patterns, the resulting ternary oxides were composed mainly of V_2MoO_8 (JCPDS: 20-1377) with some impurities of unidentified phase (Fig. 2).

After synthesis, the ternary oxides, were used either for direct nitridation or for foam preparation (Scheme 1). Scanning electron micrographs indicate significant differences in morphology between foamed and not foamed ternary oxide precursors (Fig. 1). This morphology can also play a crucial role during the nitridation process and influence the morphology of the final product. The V_3MoO_y precursor which was not foamed consists mainly of large particles that are flat on the surface (Fig. 1A,B), while the foamed substrate has a more regular structure with large amount of intrinsic porosity (Fig. 1C,D).

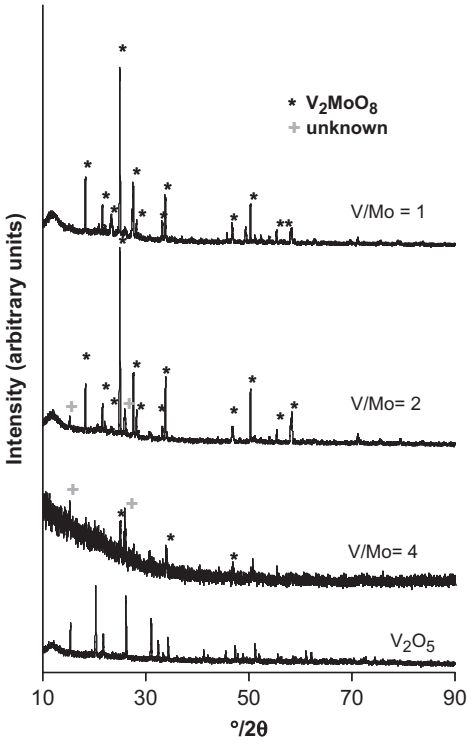

Fig. 2. X-ray diffractograms (arbitrary offset) of selected ternary V-Mo oxides with different metal stoichiometry (V/Mo ratio) and V_2O_5 precursor.

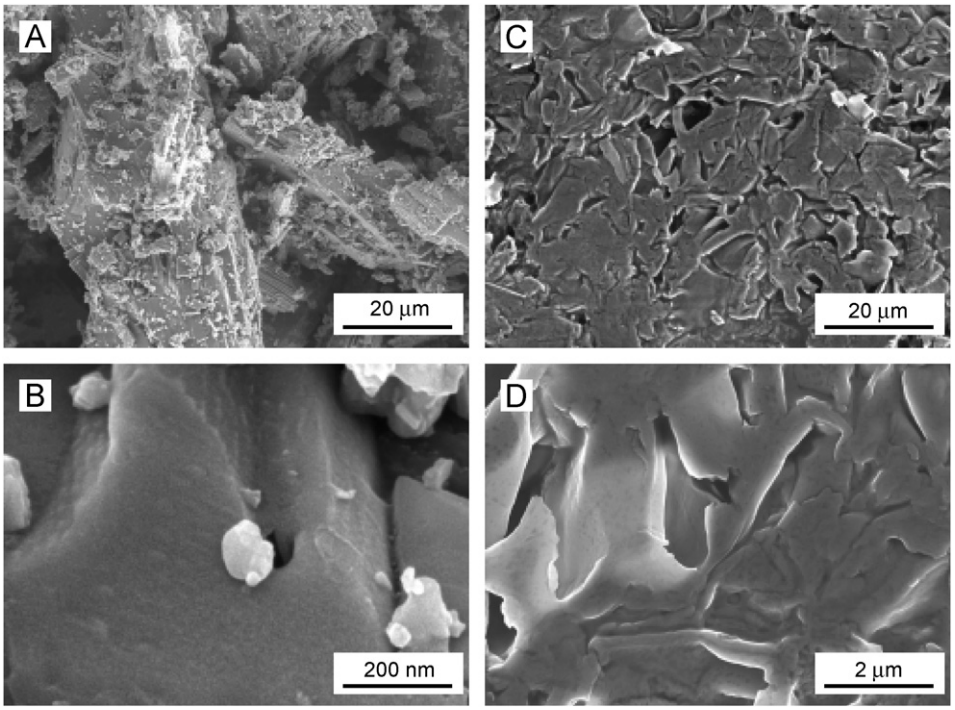

Fig. 1. Scanning electron micrographs of V_3MoO_y precursors (A, B) and corresponding foamed substrate with the same V/Mo ratio = 3 (C, D).

The ternary nitride samples prepared via foam route are marked as V_xMoN_y-FS and characterized in Table 1, while samples synthesized directly from oxides are listed in Table 2. For comparison both tables contain also the data for binary VN and Mo_2N materials synthesized for comparison (except foam derived Mo_2N-FS for which the foam synthesis was not successful-Table 1).

3.1. Specific surface area measurements

In case of foam derived materials the highest specific surface areas were observed for samples with high vanadium content (Table 1: V_4MoN_y-FS-198 $m^2 g^{-1}$). However, if the amount of molybdenum was increased, the specific surface area was decreasing (down to 45 $m^2 g^{-1}$ for the sample with the lowest vanadium content V_1MoN_y-FS). The opposite relation was observed for the materials prepared via direct nitridation procedure (Table 2). In this case, the surface area was increasing from 55 $m^2 g^{-1}$ (vanadium rich V_4MoN_y sample) to 100 $m^2 g^{-1}$, measured for V_1MoN_y sample with low vanadium content. These different relations observed for two different preparation methods of ternary V–Mo nitrides are compared in Fig. 3.

3.2. Crystallite size and X-ray diffraction measurements

For materials prepared via direct nitridation, the average crystallite diameter substantially increases with the increasing vanadium content (Table 2) (from 5.6 nm for V_1MoN_y to 16.3 nm V_4MoN_y). On the other hand, materials prepared by the foam route show only a small change in crystallite diameter as compared to significant differences in the specific surface area. Unexpectedly, the decrease of the specific surface area from 198 $m^2 g^{-1}$ (V_4MoN_y-FS) to 45 $m^2 g^{-1}$ (V_1MoN_y) corresponds to a slight decrease of the crystallite diameter from 6.1 to 3.8 nm. One reason could be the non-uniform chemical composition of nitride

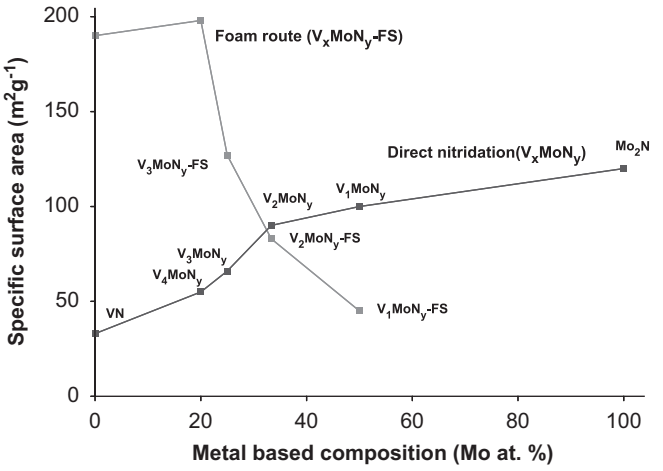

Fig. 3. Specific surface areas of ternary and binary nitrides prepared via direct nitridation (black line) and nitridation of foam derived materials via solid-state reaction route (grey line).

Table 1
Properties of ternary V–Mo nitrides prepared via the foam route

Material	Surface area[a] ($m^2 g^{-1}$)	Crystallite size[b] (nm)	Lattice constant (Å)	N content (wt%)[c]	C content (wt%)[c]	O content (wt%)[c]
VN-FS	190	6.1	4.134(15)	9.4	17.3	12.2
V_4MoN_y-FS	198	5.4	4.135(12)	10.7	4.9	32.1
V_3MoN_y-FS	127	4.3	4.137(6)	10.4	9.3	18.3
V_2MoN_y-FS	83	4.0	4.145(13)	11.2	7.5	14.1
V_1MoN_y-FS	45	3.8	4.159(5)	12.2	0.4	10.1

[a]BET specific surface area ($\pm 5\ m^2 g^{-1}$).
[b]Calculated according to the Scherrer equation [36] (± 0.6 nm).
[c]The estimated error for elemental analysis was <0.4 wt% for all measurements.

Table 2
Properties of ternary V–Mo nitrides prepared via direct nitridation

Material	Surface area[a] ($m^2 g^{-1}$)	Crystallite size[b] (nm)	Lattice constant (Å)	N content (wt%)[c]	O content (wt%)[c]
VN	33	23.0	4.113(11)	16.8	10.7
V_4MoN_y	55	16.3	4.121(3)	12.6	14.0
V_3MoN_y	66	14.7	4.121(9)	13.7	10.4
V_2MoN_y	90	13.3	4.123(12)	12.1	20.1
V_1MoN_y	100	5.6	4.130(9)	10.3	20.1
Mo_2N	120	6.0	4.191(4)	8.91	–

[a]BET specific surface area ($\pm 5\ m^2 g^{-1}$).
[b]Calculated according to the Scherrer equation [36] (± 0.6 nm).
[c]The estimated error for elemental analysis was <0.4 wt% for all measurements.

particles prepared via foam procedure (V/Mo ratio may vary in single particles). The latter will result in overlapping of measured X-ray reflections of crystallites with slightly different lattice constants contributing to the measured peak half-width. Therefore, the calculated crystallite size according to the Scherrer formula can be misleading in this case causing smaller apparent crystallite sizes. On the other hand, the low specific surface area of molybdenum-rich foam derived samples can be an effect of enhanced sintering and agglomeration.

Both γ-Mo_2N and VN crystallize in the face centered cubic unit cell (fcc) with different unit cell size. In the case of γ-Mo_2N the lattice constant is 4.197 Å while for the VN it is 4.138 Å. Ternary V–Mo nitrides were reported by Oyama to have the same fcc unit cell symmetry [25]. The V atoms are substituted by Mo in the VN crystal and Mo atoms by V in γ-Mo_2N so that VN-Mo_2N solid solutions are formed. The X-ray diffraction patterns confirmed the face centered cubic structure of ternary nitrides with peaks located in between the corresponding peaks of γ-Mo_2N and VN (Fig. 4).

Interestingly, for materials prepared via the foam procedure, different (111) and (200) peak intensity ratios were observed. In case of the samples prepared via direct nitridation, the (111) reflection had much lower intensity than (200) (Fig. 4—V_1MoN_y and V_3MoN_y), while for the foam derived samples, the (111) intensity was significantly increased (Fig. 4—V_1MoN_y-FS and V_3MoN_y-FS). Such a difference of intensity ratios was previously observed in the literature for Mo_2N with small crystallites [38]. Another possibility is that the intercalated amine can affect the anisotropic crystal growth by surface capping mechanisms.

The lattice constant increased with increasing molybdenum content. However, for foam derived ternary nitrides, the lattice constant was always higher as compared to samples prepared via direct alloy nitridation (Fig. 5), indicating incorporation of carbon into the crystal lattice. Although, carbide formation was not observed for the binary foam derived vanadium nitride sample (based on the XPS measurements), [29] the incorporation of carbon from hexadecylamine into the lattice of ternary V–Mo nitride may be possible. In contrast to vanadium (which requires temperatures higher than 1000 °C for carbide formation) Mo forms carbides (Mo_2C) as low as 600 °C [22,39]. Since all the samples prepared in this work were synthesized at 800 °C, formation of carbides in molybdenum containing samples cannot be excluded. However, for a more detailed study of carbon nature, additional measurements should be conducted (such as XPS), but this is beyond the scope of this paper.

Another reason for larger lattice constants, could be that for highly dispersed foams nitridation reaction proceeded faster than for the bulk micrometer-sized crystals of ternary oxides.

3.3. SEM and TEM of ternary nitrides

Scanning electron micrographs reveal different morphology for V_3MoN_y samples prepared via foam-route and direct nitridation (Fig. 6). The morphology of samples prepared via direct nitridation (Fig. 6C) is similar to that of the ternary oxide precursor (Fig. 1A) and consists of large particles with sharp edges. However, at higher magnification one can observe significant differences on the surface of these large particles for oxide and nitride. In case of oxide the surface if flat (Fig. 1B), while in case of nitride it particles consists of smaller crystallites with visible porosity between them (Fig. 6D).

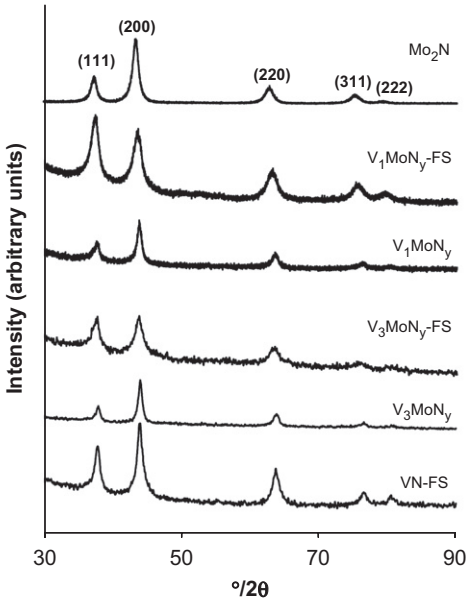

Fig. 4. X-ray diffractograms of selected ternary nitrides (foam derived—V_xMoN_y-FS and prepared via direct alloy nitridation—V_xMoN_y).

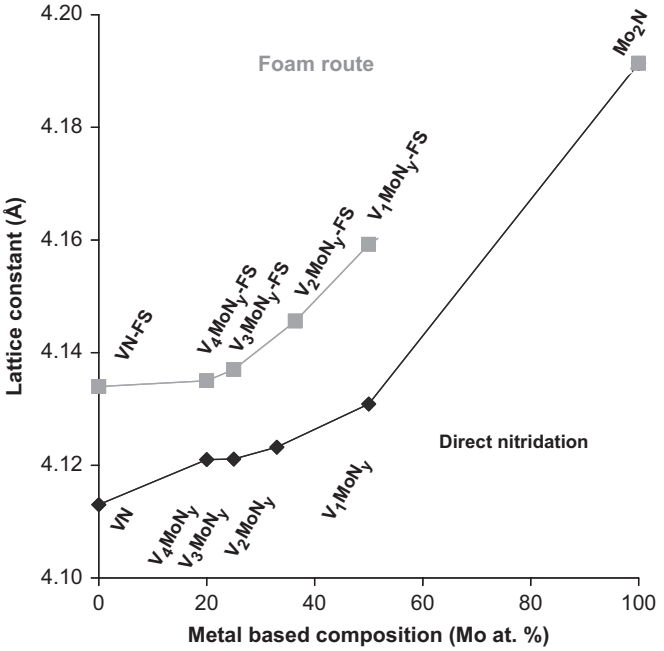

Fig. 5. Lattice constants of ternary nitrides as function of chemical composition.

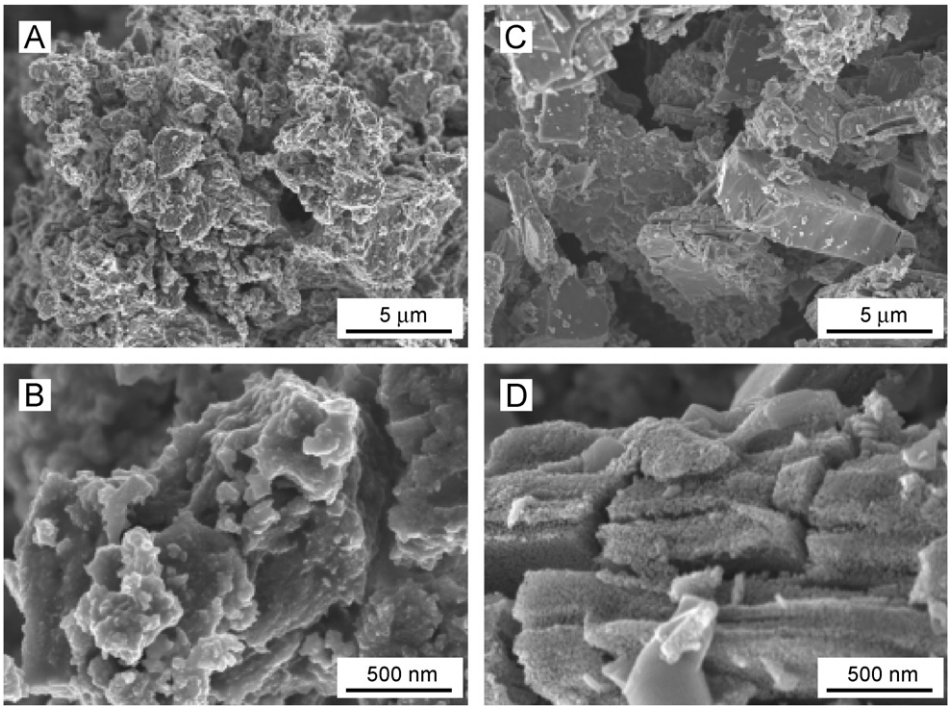

Fig. 6. Scanning electron micrographs of ternary V_3MoN_y nitride prepared via foam route (A, B) and direct nitridation (C, D).

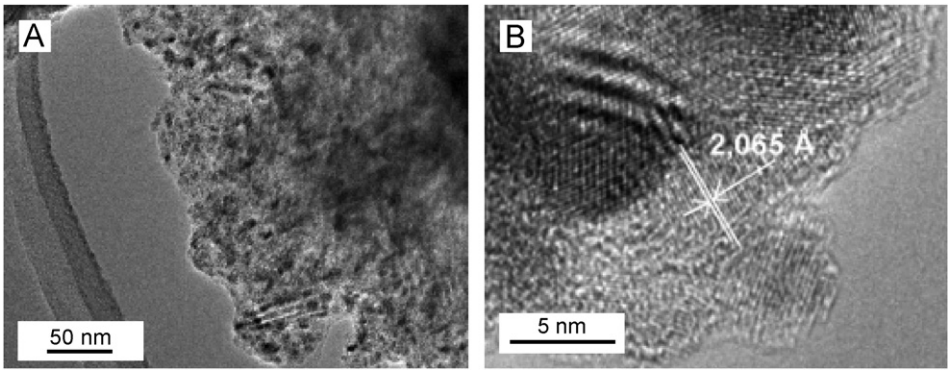

Fig. 7. (A) Transmission electron micrographs of the V_3MoN_y-FS sample prepared via foam route. (B) The measured (200) lattice spacing in nanocrystallites was 2.065 Å, while the average crystallite size was 5 nm.

For foam derived V_3MoN_y-FS material, no large particles with sharp edges could be observed, but agglomerates of smaller ones (Fig. 6A,B). This morphology is in contrast to the morphology of the oxide foam, which was more like a continuous phase and obviously was destroyed during the nitridation process (Fig. 1A, B).

TEM micrographs of V_3MoN_y-FS sample revealed agglomerates of nanocrystallites with an average diameter of 5 nm (Fig. 7A). The measured (200) lattice spacing was 2.065 Å, which corresponds to the lattice constant of 4.13 Å (Fig. 7B). No significant deviations (± 0.01 Å) were observed from this value for other particles and it corresponds well with the lattice constant calculated from the X-ray diffraction patterns.

3.4. Elemental analysis—foam derived samples

Foam derived ternary nitrides contain substantial amounts of residual carbon resulting from the amine decomposition at nitridation temperatures around 800 °C (Table 1). The highest carbon content of 17.3 wt% is detected for the sample without molybdenum (VN-FS), and the lowest of 0.4 wt% for the sample with highest molybdenum content (V_1MoN_y-FS). This means that during the nitridation in ammonia the amine could be easily removed in case of molybdenum rich samples. The latter took place most probably already at low temperatures via evaporation before decomposition took place. This indicated low degree of intercalation of amine into the precursor (for molybdenum rich samples). The carbon

content can also influence the measured specific surface areas of samples. Amorphous carbon can significantly increase the specific surface area of vanadium rich samples, however, no linear trend between carbon content and measured surface area can be observed.

For a more detailed explanation one has to analyze the oxygen content of these materials. The highest oxygen content of 32.1 wt% was observed for the V_4MoN_y-FS sample. The molybdenum containing samples are much more pyrophoric than the pure VN-FS. If exposed to air without passivation they start to glow in red, indicating very fast oxidation. Molybdenum content and specific surface area are parameters, which define the final oxygen content. On the one hand high specific surface area means smaller particles (larger contribution of oxide layer to the bulk system), while on the other hand, molybdenum doping clearly decreases the oxidation resistance. The latter is clearly visible for VN-FS and V_4MoN_y-FS materials. They possess similar specific surface area (190 and 198 $m^2 g^{-1}$, respectively) but the oxygen content is significantly different. This is the effect of much higher reactivity of V_4MoN_y-FS sample with oxygen (probably even already during the passiviation treatment). In principle the lower carbon content of this sample can also be the effect of high surface area reactivity of this sample, causing overheating and partial oxidation of carbon. Oxygen can also be located in the bulk substituting nitrogen. For other samples, the oxygen content decreases with the decreasing specific surface area (which is similar to earlier investigations for pure VN) [28].

The nitrogen content does not show significant deviations and is in the range between 9.4 (for VN-FS) and 12.2 wt% (for V_1MoN_y-FS). In principle, materials with lower specific surface area and lower carbon content have slightly higher nitrogen content (due to the lower amount of passivated oxide layer in the bulk).

3.5. Elemental analysis—samples prepared via direct nitridation

In Table 2, the nitrogen and oxygen content of materials prepared via the direct nitridation are summarized. As in the case of foam derived materials, the oxygen content increases with increasing specific surface area. However, the specific surface area for directly nitrided samples increases with the increasing molybdenum content. The nitrogen content is decreasing with the increasing molybdenum doping. This is reasonable, since molybdenum is heavier than vanadium. Moreover, molybdenum rich samples may tend to form nitrogen poor materials as in case of pure Mo_2N.

4. Conclusions

In summary, we have shown that the ternary V–Mo nitrides can be can be effectively prepared from foam precursors. This method is useful especially for materials with a high V to Mo ratio and specific surface areas are higher than for the nitrides prepared via the direct nitridation. On the other hand, for the materials with lower V to Mo ratio, the direct nitridation route seems to be preferential since higher surface areas are obtained. The preparation of foam derived nitrides was efficient and the materials obtained were crystalline according to X-ray diffraction patterns. Due to their mechanical, electronic and tribological properties, nanocrystalline nitrides may be an interesting material for applications in catalysis, electronics and composites with increased hardness or plasticity. Selected VMo_xN_y materials prepared from foams and via the direct nitridation were also preliminary tested in the propane dehydrogenation reaction. However, lower conversions and selectivities than those observed for the foam derived high surface area VN (with 190 $m^2 g^{-1}$) were measured [29]. Although the V_2O_5 foam synthesis procedure could not be directly applied for the preparation of MoO_3 foams (at least without major modification), the intercalation of amine into the molybdic acid was recently reported [40] and can be considered as an interesting substrate for the preparation of the high surface area molybdenum nitride or carbide.

Acknowledgment

Support from the German Research Foundation (KA 1698/1-1, WE 874/18-1) is gratefully acknowledged.

References

[1] W. Lengauer, Handbook of Ceramic Hard Materials, vol. 1, Wiley-VCH, Weinheim, 2000 (Chapter 7).
[2] W.S. Williams, JOM 49 (1997) 38–42.
[3] R. Sanjines, P. Hones, F. Levy, Thin Solid Films 332 (1998) 225–229.
[4] D. Choi, G.E. Blomgren, P.N. Kumta, Adv. Mater. 18 (2006) 1178.
[5] R.B. Levy, M. Boudart, Science 181 (1973) 547–549.
[6] L. Volpe, S.T. Oyama, M. Boudart, Stud. Surf. Sci. Catal. 16 (1983) 147–158.
[7] S.T. Oyama, Catal. Today 15 (1992) 179–200.
[8] S.T. Oyama, The Chemistry of Transition Metal Carbides and Nitrides, Blackie Academic & Professional, London, 1996 'Vol.' Chapter 1.
[9] E. Furimsky, Appl. Catal. A:Gen. 240 (2003) 1–28.
[10] S.Z. Li, J.S. Lee, T. Hyeon, K.S. Suslick, Appl. Catal. A: Gen. 184 (1999) 1–9.
[11] M. Nagai, T. Suda, K. Oshikawa, N. Hirano, S. Omi, Catal. Today 50 (1999) 29–37.
[12] D. Farrusseng, K. Schlichte, B. Spliethoff, A. Wingen, S. Kaskel, J.S. Bradley, F. Schüth, Angew. Chem. Int. Ed. 40 (2001) 4204–4207.
[13] S. Kaskel, K. Schlichte, B. Zibrowius, Phys. Chem. Chem. Phys. 4 (2002) 1675–1681.
[14] S. Kaskel, K. Schlichte, G. Chaplais, M. Khanna, J. Mater. Chem. 13 (2003) 1496–1499.
[15] G. Chaplais, K. Schlichte, O. Stark, R.A. Fischer, S. Kaskel, Chem. Commun. (2003) 730–731.
[16] J.R. Groza, Nanostruct. Mater. 12 (1999) 987–992.
[17] J.R. Groza, Int. J. Powder Metall. 35 (1999) 59–66.
[18] M. Mitomo, Y.W. Kim, H. Hirotsuru, J. Mater. Res. 11 (1996) 1601–1604.
[19] J.G. Choi, J. Ha, J.W. Hong, Appl. Catal. A-Gen. 168 (1998) 47–56.

[20] T. Kadono, T. Kubota, Y. Okamoto, Catal. Today 87 (2003) 107–115.
[21] R. Kapoor, S.T. Oyama, J. Solid State Chem. 99 (1992) 303–312.
[22] Y.J. Zhang, Q. Xin, I. Rodriguez-Ramos, A. Guerrero-Ruiz, Mater. Res. Bull. 34 (1999) 145–156.
[23] Z.B. Wei, Q. Xin, P. Grange, B. Delmon, J. Catal. 168 (1997) 176–182.
[24] C.C. Yu, S. Ramanathan, F. Sherif, S.T. Oyama, J. Phys. Chem. 98 (1994) 13038–13041.
[25] C.C. Yu, S.T. Oyama, J. Solid State Chem. 116 (1995) 205–207.
[26] S.T. Oyama, R. Kapoor, H.T. Oyama, D.J. Hofmann, E. Matijevic, J. Mater. Res. 8 (1993) 1450–1454.
[27] S. Alconchel, F. Sapina, D. Beltran, A. Beltran, J. Mater. Chem. 9 (1999) 749–755.
[28] O. Merdrignac-Conanec, K. El Badraoui, P. L'Haridon, J. Solid State Chem. 178 (2005) 218–223.
[29] P. Krawiec, P.L. De Cola, R. Gläser, J. Weitkamp, C. Weidenthaler, S. Kaskel, Adv. Mater. 18 (2006) 505–508.
[30] A. Fischer, M. Antonietti, A. Thomas, Adv. Mater. 19 (2007) 264–267.
[31] H.Z. Zhao, M. Lei, X. Yang, J.K. Jian, X.L. Chen, J. Am. Chem. Soc. 127 (2005) 15722–15723.
[32] B. Song, J.K. Jian, G. Wang, M. Lei, Y.P. Xu, X.L. Chen, Chem. Mater. 19 (2007) 1497–1502.
[33] G.T. Chandrappa, N. Steunou, J. Livage, Nature 416 (2002) 702.
[34] O. Durupthy, M. Jaber, N. Steunou, J. Maquet, G.T. Chandrappa, J. Livage, Chem. Mater. 17 (2005) 6395–6402.
[35] F. Carn, N. Steunou, J. Livage, A. Colin, R. Backov, Chem. Mater. 17 (2005) 644–649.
[36] STOE Size/Strain analysis software with implemented Scherrer equation (WinXPOW), 1.06; STOE WinXPOW: 1999.
[37] I.M. Arabatzis, P. Falaras, Nano Lett. 3 (2003) 249–251.
[38] R.N. Panda, S. Kaskel, J. Mater. Sci. 41 (2005) 2465–2470.
[39] X.H. Wang, H.L. Hao, M.H. Zhang, W. Li, K.Y. Tao, J. Solid State Chem. 179 (2006) 538–543.
[40] M.I. Shukoor, H.A. Therese, L. Gorgishvili, G. Glasser, U. Kolb, W. Tremel, Chem. Mater. 18 (2006) 2144–2151.